Image Cover Sheet

CLASSIFICATION	SYSTEM NUMBER	500380
UNCLASSIFIED		

TITLE

REMOTE DETERMINATION OF CLOUD TEMPERATURE AND TRANSMITTANCE FROM
SPECTRAL RADIANCE MEASUREMENTS: METHOD AND RESULTS

System Number:

Patron Number:

Requester:

Notes:

DSIS Use only:

Deliver to: FF

UNCLASSIFIED

DEFENCE RESEARCH ESTABLISHMENT
CENTRE DE RECHERCHES POUR LA DÉFENSE
VALCARTIER, QUÉBEC

DREV - R - 9608

Unlimited Distribution / Distribution illimitée

REMOTE DETERMINATION OF
CLOUD TEMPERATURE AND TRANSMITTANCE FROM
SPECTRAL RADIANCE MEASUREMENTS:
METHOD AND RESULTS

by

Jean-Marc Thériault

October / octobre 1996

Approved by / approuvé par

Chief Scientist / Scientifique en chef

1 Nov, 1996
Date

SANS CLASSIFICATION

i

ABSTRACT

In this report a method for the evaluation of cloud temperature and transmittance from ground-based measurements of the downwelling spectral radiance is proposed. The method uses the strong emission band of ozone at 9.6 µm, which constitutes a natural source of IR radiation for probing clouds. Temperature and transmittance are derived from the cloudy sky radiance measured in two narrow spectral channels : The first one is approximately at the center of the ozone band at 9.48 µm and the second one is off the band at 9.15 µm. The cloud parameters are found by solving a system of equations requiring, as input, an estimate of the cloud height and thickness obtained from lidar returns, and of atmospheric temperature and humidity profiles. The validation tests performed on experimental spectra demonstrate the accuracy of the method with typical temperature errors smaller than 2 K for the spectral measurements coincident in time with the lidar measurements. Finally, the main sources of method limitation are identified and analyzed.

RÉSUMÉ

Dans ce rapport, on propose une méthode d'évaluation de la température et de la transmittance des nuages en se basant sur des mesures de radiance spectrale effectuées au niveau du sol. Cette méthode tire avantage du fait qu'il y a une forte bande d'émission de l'ozone à 9.6 µm, ce qui constitue une source naturelle de rayonnement infrarouge pour le sondage des nuages La température et la transmittance sont évaluées à partir de la radiance du ciel nuageux mesurée dans deux régions spectrales étroites: la première se trouve approximativement au centre de la bande d'ozone à 9.48 µm et la seconde, à l'extérieur de cette bande à 9.15 µm. Les paramètres du nuage sont résolus à partir d'équations qui nécessitent une estimation de la hauteur et de l'épaisseur du nuage, et des profils de température et d'humidité. Les tests de validation effectués sur des spectres expérimentaux démontrent la précision de la méthode proposée, avec des erreurs typiques de température plus petites que 2 K dans le cas où les mesures spectrales sont en coïncidence temporelle avec les mesures du lidar. Finalement, les principales sources de limitation de la méthode sont identifiées et analysées.

UNCLASSIFIED

iii

TABLE OF CONTENTS

UNCLASSIFIED

v

EXECUTIVE SUMMARY

The Canadian Forces are using an increasing number of electro-optical systems for the remote sensing of target characteristics and other information of military interest. Defence Research Establishment Valcartier (DREV) has been involved in remote sensing for many years, especially in the field of lidars and Fourier Transform Infra-Red (FTIR) spectrometers. Recently, DREV has demonstrated a new multiple-field-of-view lidar technique for the remote sensing of atmospheric aerosols. DREV is also developing a new FTIR technique for the remote sensing of atmospheric parameters, such as temperature and humidity profiles.

One application for which these two DREV techniques appear particularly promising is the remote sensing of icing hazard conditions. The military and commercial aviation communities are very concerned with this problem since more than thirty-five aircraft accidents are reported each year in North America. Aircraft-icing conditions happen in a cloud composed of large water droplets at temperature below freezing point. In this context, we have recently started a feasibility study of an on-board lidar-radiometer system for mapping icing conditions. The first step of this project consisted in performing simultaneous lidar and spectral measurements (FTIR) to develop a method for determining cloud temperature and composition: ice crystals or supercooled water droplets. Lidar data can provide information on particle size and concentration while spectral data contains information on cloud temperature.

The purpose of this report is to present a new method for the remote determination of cloud temperature and transmittance. The method is founded on passive measurements of the downwelling spectral radiance coming from the cloud. This development is supported by ground-based observations performed with a FTIR spectrometer having a spectral resolution of 1 cm^{-1} and covering the infrared (IR) band from 3 to 20 μm. The cloud evaluation method uses the strong emission band of ozone in the IR spectral range. Because most of the ozone emission originates from the upper atmosphere, it constitutes a natural source of IR radiation for probing clouds in the lower part of the atmosphere using a ground-based receiver. The solution for cloud temperature and transmittance is found by solving a system of equations that requires an estimate of cloud height and thickness obtained from lidar returns, and an estimate of atmospheric temperature and humidity profiles for calculations of the atmospheric background. The method has been successfully tested on experimental spectra. It was found that temperature errors are typically smaller than 2° C when spectral measurements are coincident in time with the lidar measurements. The main sources of errors have been identified and their impact on the accuracy of the method has been addressed. The next steps will focus on generalizing the cloud evaluation method to any slant paths from the ground or from an airborne platform.

This report presents a basis to further develop the cloud evaluation method for applications in icing hazard detection. The ultimate goal is to demonstrate that combined lidar and spectral measurements (two bands) can be used for determining the temperature of a cloud and whether it is made of ice crystals or super-cooled water droplets. The results of this work may also apply to other domains in which remote sensing techniques are utilized such as in cloud microphysics, climatology and meteorology. Finally, this work contributes directly to Canadian inputs to TTCP JTP-13.

UNCLASSIFIED

1

1.0   INTRODUCTION

The Canadian Forces are using an increasing number of passive and active electro-optical (EO) sensors to assist military units in performing tasks such as surveillance, detection, identification and designation. The continuous effort for improving sensors' performance has favored the development of many sectors of science and technology. One sector that has experienced very rapid and successful developments is remote sensing. For many years, Defence Research Establishment Valcartier (DREV) has been deeply involved in this field of research, especially in the development and exploitation of two specific technologies: lidar and Fourier Transform Infra-Red (FTIR) spectrometer. In the case of lidar, DREV has recently proposed and demonstrated a new multiple-field-of-view (MFOV) lidar technique for the remote sensing of atmospheric aerosols (Ref. 1). In the case of an FTIR spectrometer, DREV has been developing a new technique for the remote sensing of atmospheric parameters such as temperature and humidity profiles (Ref. 2).

One application for which these two techniques (MFOV lidar and FTIR spectrometer) appear particularly promising is for the remote sensing of icing hazard conditions for aircrafts. The military and commercial aviation communities are very concerned with this problem: In North America, more than 400 aircraft accidents due to icing have been reported since 1975 (Ref. 3). Basically, aircraft-icing conditions happen in a cloud composed of large water droplets found at temperature below freezing point. In this context, DREV has initiated a feasibility study of an on-board lidar-radiometer system for mapping icing conditions. The first step of this project consists in performing a series of simultaneous lidar and spectral measurements (FTIR) to develop a method for determining cloud temperature and composition, i.e. ice crystals or supercooled water droplets. Lidar data can provide information on the particles' size and composition, while spectral data contain information on cloud temperature.

The purpose of this report is to develop and verify a new method for the remote determination of cloud temperature. The method is founded on ground-based measurements of the downwelling spectral radiance coming from the cloud. In Chapter 2 the FTIR spectrometer is described, while Chapter 3 presents recent field measurements of the downwelling spectral radiance for different cloud conditions. It is shown that the FTIR technique is particularly efficient in observing cloud emission and scattering because of its high sensitivity, very wide spectral coverage and spectral resolution. In Chapter 4 the

UNCLASSIFIED

2

cloud evaluation method is formulated: The cloud temperature and IR transmittance (9.3 μm) are derived from the cloudy sky radiance measured in two narrow spectral channels. Theoretical and experimental verifications of the method are reported in Chapter 5 together with an evaluation of the two main sources of errors. Finally, Chapter 6 summarizes the work and draws conclusions on the perspective of extending the cloud evaluation method to scenarios involving airborne measurements.

This work was performed at DREV between June 1995 and May 1996 under Thrust 3.D - Airborne Search and Localization, Work Unit 03D03-15: Icing Hazard Detection.

2.0 DESCRIPTION OF THE SPECTROMETER SYSTEM

The method for remotely evaluating cloud temperature and transmittance is founded on the ground-based measurement of the IR radiation emitted by the cloud and the surrounding atmosphere. For the present study, the ground-based measurements were taken with a DREV-designed Fourier spectrometer referred to as the Double Beam Interferometer Sounder (DBIS).

Essentially, the DBIS is made of one or, optionally, two 10-in. diameter Cassegrain telescopes optically coupled to a double-input port Fourier transform spectrometer and two detection units (output optics 1 and 2). Figure 1 summarizes the design of the instrument. Note that only one telescope assembly is explicitly shown in Fig. 1. This instrument allows for measurements of calibrated spectra according to the following specifications: any selectable zenith angle, scene FOV of 5 mrad, spectral coverage from 3 to 20 μm and a spectral resolution of 1 cm^{-1} or greater. As part of the input modules, a large flat plate mirror placed in front of the telescope can be either rotated to the selected scene or oriented in a position for the acquisition of reference spectra. The pointing capability of this scene mirror makes it possible to take slant path measurements from 0 to 360 degrees with a tilt adjustment of ± 10 degrees in azimuth and an accuracy of 0.1 degree. The coarse adjustment in azimuth is simply achieved by rotating the whole assembly mounted on a turn table. After reflection on the scene mirror, the beam is then successively focussed by the Cassegrain telescope and reflected by an off-axis parabolic mirror (PM) to produce a collimated beam of appropriate diameter at the input-port of the interferometer. The two output modules are identical, except that channel 1 includes an MCT detector (HgCdTe) optimized for the
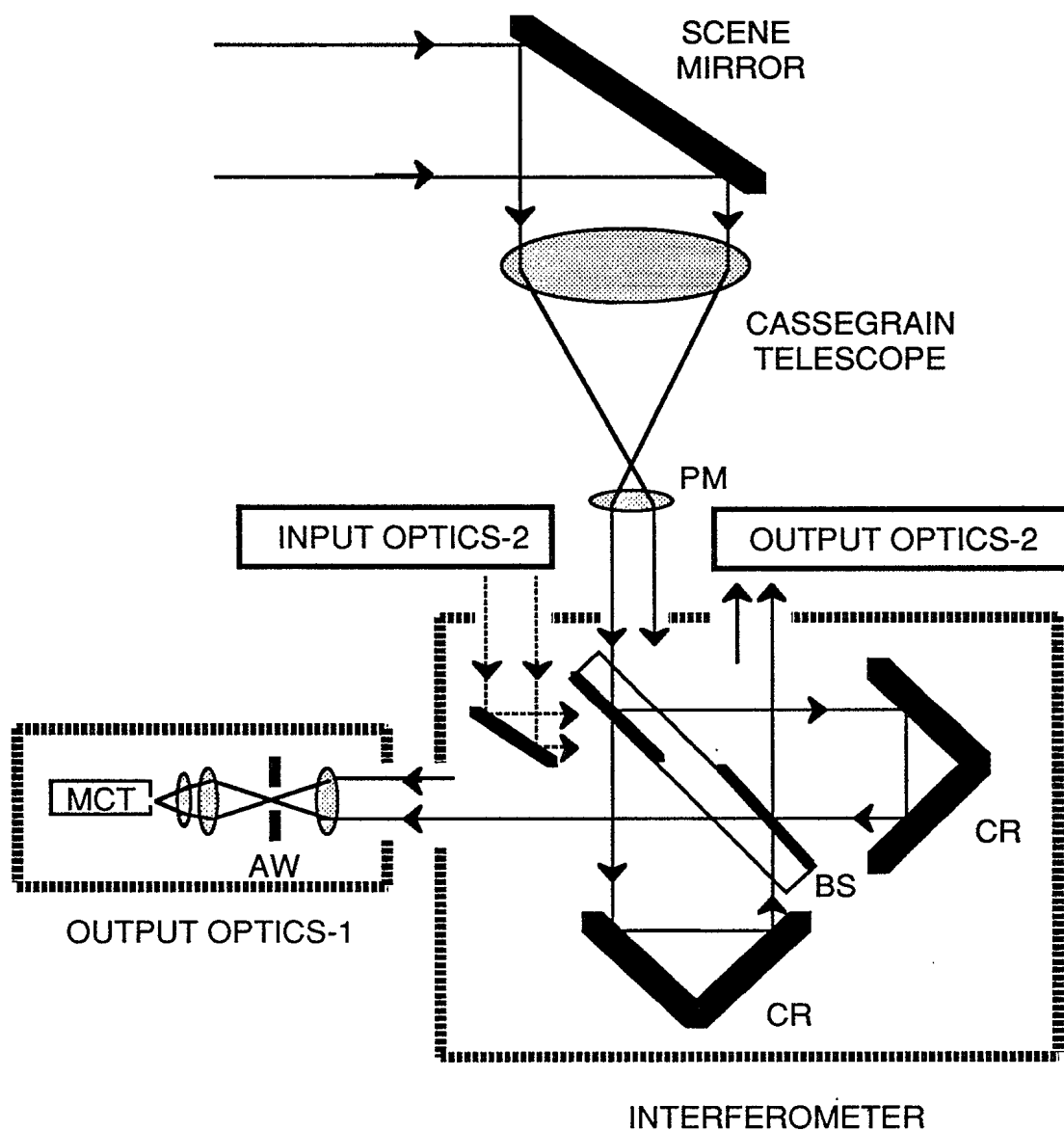
3

FIGURE 1 - Schematic representation of the Fourier spectrometer system referred to as the Double input Beam Interferometer Sounder (DBIS)

4

5-20 μm spectral region, while channel 2 includes an InSb detector optimized for the 2-5 μm region. Note that the InSb module is not explicitly shown in Fig. 1. These modules contain parabolic and condensing mirrors that focus the beam coming from the interferometer onto a detector (MCT or InSb) of 1 mm diameter. An aperture wheel (AW) mounted with stops of different diameters allows for the adjustment of the field of view (FOV) of the instrument (5 mrad or smaller). A camera boresighted to the telescope can be used to aim and visualize the measured scene.

The spectrometer is a standard BOMEM MB100 field interferometer that uses corner reflectors rather than the usual flat plate mirrors normally utilized in the Michelson configuration. With such an interferometer, two beams coming from different scenes and entering different input ports (one or two) can be optically combined and spectrally subtracted in real time. Basically, this capability arises from the fact that the two interferograms associated to each input port are out of phase. However, in this study, measurements were taken with the single telescope configuration, where in this case the second telescope is replaced by a stable cold blackbody (liquid nitrogen; Input Optics-2).

The radiometric calibration of DBIS spectra is based on the two-temperature method. Two temperatures are required because there are two unknowns: the gain and the offset (self emission) of the instrument. To this end, two large flat plate blackbodies (12"x12") kept at constant temperatures have been used: one referred to as the hot blackbody is stabilized at a temperature of 40° C, while the other referred to as the ambient blackbody is stabilized at a temperature near the ambient temperature of operation (~ 10 to 25° C). The accuracy of both blackbodies is of the order of 0.1° C. To obtain a calibrated emission spectrum, three measurements are required: the raw spectrum corresponding to the emission of the atmosphere and two raw spectra from the reference blackbodies. Each raw spectrum is obtained by coadding 20 individual scans taken at a resolution of 1 cm^{-1}. In these conditions of operation, the Root Mean Square (RMS) noise has been measured to be smaller than 0.2 K (brightness temperature) almost everywhere in the usable portion of the 3-20 μm region.

UNCLASSIFIED

5

3.0 ATMOSPHERIC EMISSION SPECTRA: RESULTS

Examples of downwelling emission spectra (zenith angle = 0 degree) expressed in brightness temperature appear in Figs. 2 and 3. The brightness temperature T_B is simply obtained by inverting the Planck radiance equation

$$T_B(\nu) = \frac{1.439\,\nu}{\ln\left(\dfrac{1.191 \times 10^{-12}\,\nu^3}{R(\nu)} + 1\right)},$$

where numerical constants are defined to match the radiance spectrum $R(\nu)$ (watts / cm^2-ster-cm^{-1}) with the temperature unit (K) assuming a wavenumber ν in cm^{-1}. The upper curve of Fig. 2 corresponds to a typical spectral radiance measured in clear sky conditions. For comparison purposes, the bottom curve represents the corresponding calculation performed with a recent version of the FASCOD3 model (Ref. 7). Radiosonde profiles of pressure, temperature and humidity have been used as input for calculations together with a clear midlatitude summer atmosphere for the other species. Typically, clear sky calculations adequately reproduce the measurements. Spikes appearing in the 1500-1800 cm^{-1} region and near 660 cm^{-1} in the measured spectrum of Fig. 2 are essentially artefacts due to limitations in the calibration procedure when applied to very strong absorption bands.

The general shape of clear sky spectra is dominated by the temperature and the absorption properties of the constituents along the optical path. In spectral regions where absorption is strong, the atmosphere radiates its energy like a blackbody at a temperature roughly equal to that near the sounder. This is observed in the two strong absorption bands of CO_2 near 15 μm (660 cm^{-1}) and 4.3 μm (2325 cm^{-1}), and also in the 1400-1800 cm^{-1} region (6.3 μm) where the absorption is mainly due to water vapor. If we exclude the important emission band of the O_3 near 9.6 μm (1040 cm^{-1}), the atmospheric window region from 800 to 1200 cm^{-1} (8-12 μm) is dominated by the water vapor absorption lines (fine spectral structure) and continuum (smooth spectral shape).

Figure 3 compares radiances associated to clear and cloudy skies. For instance, curve 2 represents typical emission spectra for a sky having a thin cloud of moderate transparency at an altitude of approximately 1.4 km. In this case, the radiance recorded in the 8 to 12 μm region (800-1200 cm^{-1}) is largely dominated by the cloud emission, while in the 3-4 μm
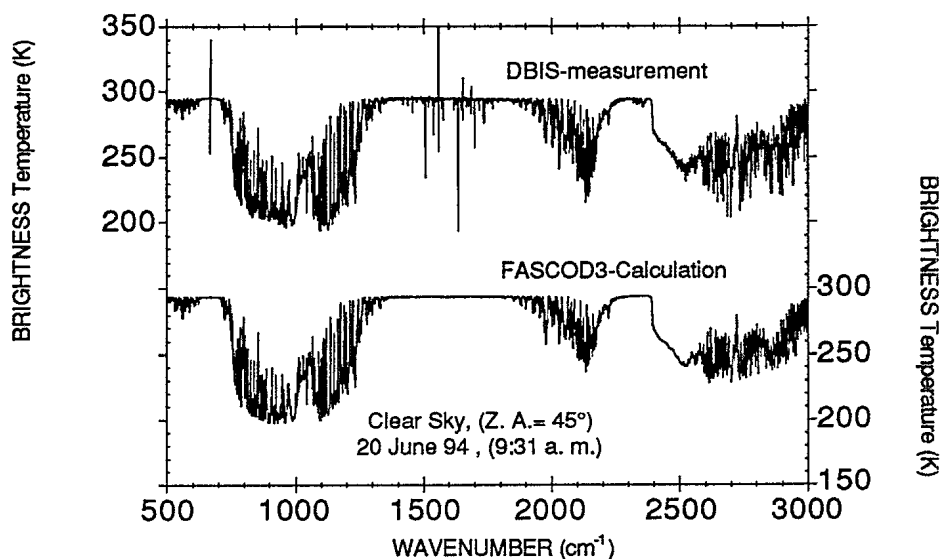
FIGURE 2 - Typical example of spectra measured with the DBIS and calculated with FASCOD3 for a clear day corresponding to midlatitude summer conditions
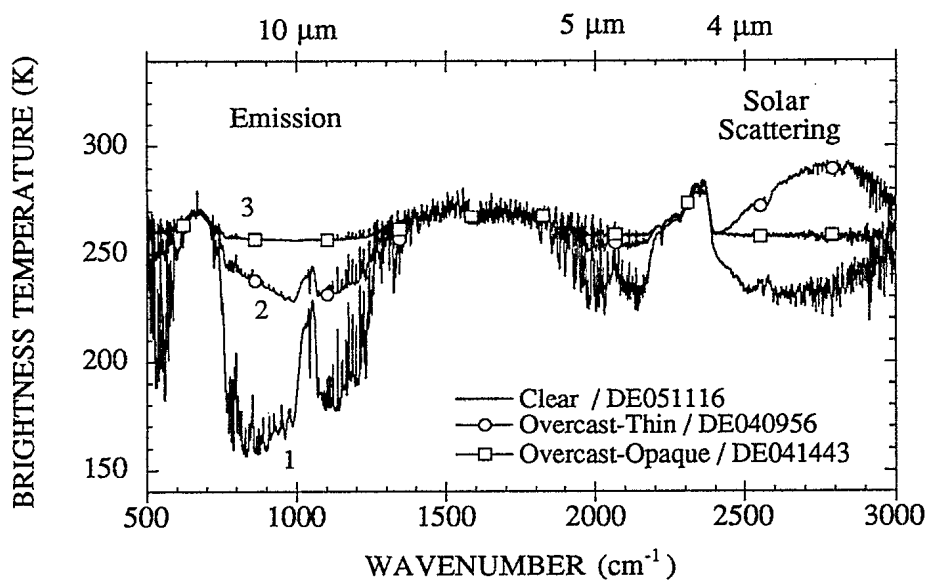
FIGURE 3 - Typical ground-based measurements of the downwelling spectral radiance for three atmospheric conditions: clear sky (curve 1), thin transparent cloud (curve 2), and opaque cloud (curve 3)

region the dominant radiance contribution is due to solar scattering on cloud particles. Curve 3 represents approximately the same situation as in curve 2, except that the cloud layer is opaque. In this case the solar scattering component in the 3-4 μm region disappears due to large cloud extinction and cloud emission becomes the dominant contribution.

4.0 METHOD OF CLOUD EVALUATION

Ground-based observations of cloud emissions in the IR has prompted the development of a simple spectral method for estimating the transmittance (at 9.3 μm) and the apparent temperature of a cloud layer. Figure 4 introduces the method where three radiance spectra recorded in the 8 to 12 μm window are compared for different sky conditions: clear, thin cloud and opaque cloud. As seen, the cloud amount tends to decrease the contrast of the ozone emission band near 9.6 μm and the cloud temperature tends to increase the overall emission in the window. To take advantage of this behavior and retain the benefit of a simple estimation procedure, two narrow spectral channels have been selected (vertical bars in Fig. 4). The choice of this pair is not arbitrary. Channel 1 corresponds to a wavelength of 9.48 μm ($1054-1055$ cm^{-1}): It is used to probe the ozone signal and is free of absorption lines. Channel 2 corresponds to a wavelength of 9.15 μm ($1093-1094$ cm^{-1}): It depends essentially on the water vapor continuum and is also free of absorption lines. Because the mixing ratio of the ozone peaks at an altitude of 27 km, an important part of the ozone emission (channel 1) occurs above cloud layers. Consequently, the signal received on channel 1 is mainly due to the ozone emission attenuated by the cloud layer. Channel 2 may be seen as a probe for the apparent temperature . Also shown in Fig. 4 are the absorption coefficients of liquid water and ice crystal. These indicate that water clouds and ice clouds should have approximately the same optical properties near the 9.3 μm spectral region. In the 11-12 μm region, distinct ice and water coefficients would impact differently the resulting radiance.

In Fig. 5, the bulk reflectance of liquid water and ice crystal are compared. The low reflectance values (~ 1 %) in the region of the two probing channels indicate that the scattering process inside the cloud is dominated by absorption and transmission mechanisms. This constitutes an advantage in the proposed method because it is assumed that earth IR emission reflected down by the cloud can be neglected, which greatly simplifies the equations of the method (as seen below).
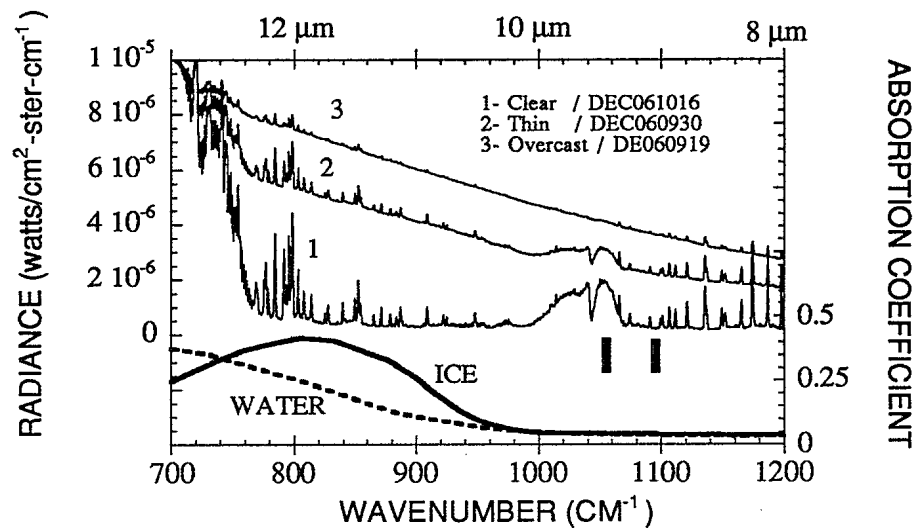
8

FIGURE 4 - Spectral radiances for three different sky conditions (upper curves, left scale). Absorption coefficients of liquid water and ice cristal (bottom curves, right scale). Vertical bars correspond to two narrow channels selected for cloud temperature and transmittance evaluations
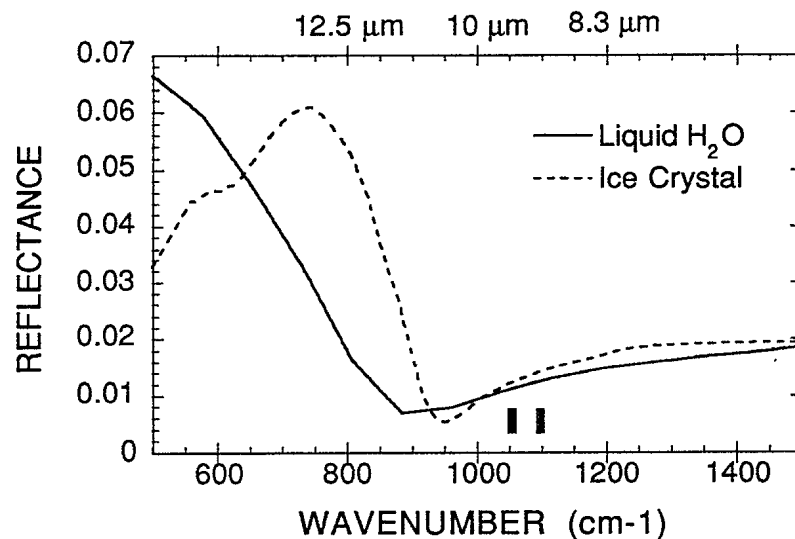

FIGURE 5 - Bulk reflectance of liquid water and ice cristal. The two vertical bars correspond to the narrow channels selected for cloud temperature and transmittance evaluation

UNCLASSIFIED

9

In the following, the equations of the method are developed in relation with the atmospheric layering depicted in Fig. 6. For a plane-parallel clear atmosphere (Fig. 6a) in local thermodynamic equilibrium with no scattering, the downwelling spectral radiance $R(v)$ may be expressed in terms of three components:

$$R(v) = u_{L+1}(v)\, \tau_{L+1} + B(v)\left[1 - \tau^m(v)\right]\tau_L(v) + D_L(v) \tag{1}$$

where L is an arbitrary level, $u_{L+1}(v)$ corresponds to the downwelling radiance measured at level L+1, $\tau^m(v)$ is the molecular transmittance of the layer L, $\tau_L(v)$ is the transmittance from level L to the ground, $B(v)$ is the Planck radiance associated to layer L and $D_L(v)$ corresponds to the radiance of the atmosphere below level L. Similarly, the downwelling radiance $R'(v)$ of an atmosphere containing a cloud layer at level L (Fig. 6b) is given by

$$R'(v) = u_{L+1}(v)\, \tau_{L+1}(v)\, \tau^c + B(v)\left[1 - \tau^c\tau^m(v)\right]\tau_L(v) + D_L(v) \tag{2}$$

where τ^c is defined as the transmittance of the cloud layer, $[1 - \tau^c\tau^m(v)]\, B(v)$ is the associated gray body radiance of the cloud. It is important to note that the Planck radiance terms $B(v)$ in eqs. 1 and 2 are assumed to be identical. Also note that in eq. 2, the cloud reflected radiation coming from the earth emission and the surrounding atmosphere is neglected. This represents a good approximation because of the low reflectance of liquid water and ice crystal in the spectral region near 9.3 µm. Inserting the clear sky radiance eq. 1 into eq. 2 for the two probing channels, v_a (1054-1055 cm^{-1}) and v_b (1093-1094 cm^{-1}) and assuming that τ^c is the same for the two channels yields the following system of equations:

$$R'(v_a) - R(v_a) = (1 - \tau^c)\left[\, B(v_a) - u_{L+1}(v_a)\,\right]\tau_{L+1}(v_a) \tag{3}$$

$$R'(v_b) - R(v_b) = (1 - \tau^c)\left[\, B(v_b) - u_{L+1}(v_b)\,\right]\tau_{L+1}(v_b) \tag{4}$$

These equations were obtained using the expression for the transmittance $\tau_{L+1} = \tau^m\,\tau_L$.

The two unknowns to be solved are τ^c and B. Other quantities are properly estimated based on clear sky radiance measurements or calculations, associated radiosonde or inverted profiles and radiative transfer calculations to evaluate u_{L+1} and τ_{L+1}. For a given temperature, the Planck radiances $B(v_a)$ and $B(v_b)$ evaluated at two arbitrary wavenumbers are related to each other by the general expression:
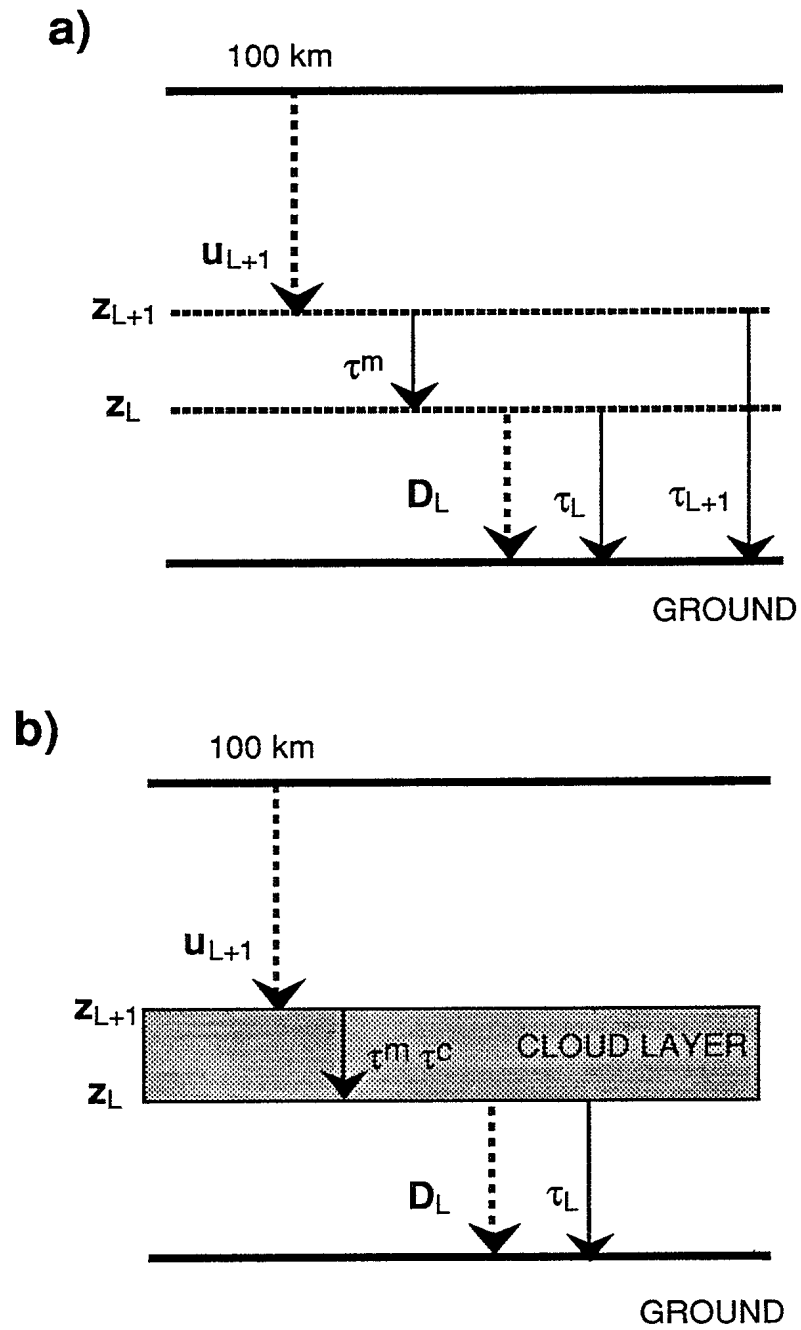
10

FIGURE 6 - Atmospheric layering related to the method for cloud temperature and transmittance evaluation: a- clear atmosphere; b- atmosphere with a cloud layer

UNCLASSIFIED

11

$$B(\nu_b) = \frac{c\,\nu_b^3}{1+\left(1+c\,\frac{\nu_a^3}{B(\nu_a)}\right)^{\frac{\nu_b}{\nu_a}}},$$ [5]

where the constant $c = 1.191 \times 10^{-12}$. In the case of the two probing channels selected for the present method, ν_a (1054-1055 cm^{-1}) and ν_b (1093-1094 cm^{-1}), eq. 5 reduces to

$$B(\nu_b) = 1.42198\,[B(\nu_a)]^{(1.03698)},$$ [6]

and eqs. 3 and 4 can be combined to eliminate the unknown transmittance τ^c, which gives a simple expression for $B(\nu_a) = B_a$

$$C_1\,(B_a)^{1.03698} + C_2\,(B_a) + C_3 = 0,$$ [7]

where

$$C_1 = 1.42198\,m\,\tau_{L+1}(\nu_b),$$
$$C_2 = -\,\tau_{L+1}(\nu_a),$$
$$C_3 = u_{L+1}(\nu_a)\tau_{L+1}(\nu_a) - m\,u_{L+1}(\nu_b)\tau_{L+1}(\nu_b).$$

and

$$m = \frac{R'_a - R_a}{R'_b - R_b}.$$

B_a is found by solving eq. 7 numerically using the Newton method. In this case, the initial solution B^0_a is found by assuming that $B_a = B_b$ in eqs. 3 and 4. The solution (one iteration) is given by

$$B_a = B^0_a - \frac{F(B^0_a)}{F'(B^0_a)},$$ [8]

where

$$F(B^0_a) = C_1\,(B^0_a)^{1.03698} + C_2\,(B^0_a) + C_3,$$
$$F'(B^0_a) = 1.03698C_1\,(B^0_a)^{0.03698} + C_2,$$

and

12

$$B_a^0 = \frac{-C_3}{\dfrac{C_1}{1.42198} + C_2}.$$

Knowing B_a, it is easy to solve analytically for τ^c, which can be obtained from

$$\tau^c = 1 - \left(\frac{R'_a - R'_b - R_a + R_b}{C_4 - C_5} \right), \qquad [9]$$

with

$$C_4 = [\, B_a - u_{L+1}(\nu_a) \,]\, \tau_{L+1}(\nu_a),$$

and

$$C_5 = [\, B_b - u_{L+1}(\nu_b) \,]\, \tau_{L+1}(\nu_b).$$

Equations 7 and 9 summarize the result of the cloud evaluation method. The apparent temperature of the cloud layer is simply found by inverting the Planck radiance solved at eq. 7. It depends on the measured radiances of the cloudy skies R'_a and R'_b, and the calculated (or measured) radiances of the associated clear skies R_a and R_b. The IR transmittance of the cloud at 9.3 μm is estimated by eq. 9 and depends on the Planck radiances of the clouds B_a and B_b (found by eq. 7), the measured radiances of the cloudy skies R'_a and R'_b and the calculated (or measured) radiances of the associated clear skies R_a and R_b. The constants C_1, C_2, C_3, C_4 and C_5 are computed with MODTRAN based on radiosonde or inverted profiles obtained from the current or a representative clear sky condition.

5.0 RESULTS AND ANALYSES

Verifications of the cloud evaluation method have been performed on a case (6 December 1995) in which coincident radiance, radiosonde and lidar data were recorded. The radiosonde launch site was located at Canadian Forces Base Valcartier (3 km from DREV), while the site for spectral and lidar measurements was located at DREV. Typically, radiosondes were launched once a day at 09:30 a.m. local time. For the 6 December case the temperature at ground level was 271 K and the sky was totally covered by a cloud layer of variable opacity. Inspection of the lidar returns indicates a cloud base at an altitude of 1.4 km and a cloud thickness of approximately 0.4 km. At this altitude range (1.4-1.8 km) the radiosonde data exhibit a very weak temperature inversion, averaging around 260 K. This

UNCLASSIFIED

13

corresponds to the apparent temperature of the cloud since the atmosphere is assumed to be in thermal equilibrium.

5.1 Verification of the Method

A first verification of the method was achieved on simulations. They were calculated with a version of the radiative transfer model MODTRAN2. For that, meteorological parameters for model calculations correspond to the radiosonde temperature and humidity profiles (6 December 1995), while other needed profiles for the dry atmosphere correspond to midlatitude winter conditions. Based on these profiles, MODTRAN2 was run in two consecutive steps to generate all the required input to verify the method (eqs. 7 and 9). At the first step, MODTRAN2 was used to compute the clear sky transmittance τ_{L+1} from level L+1 to the ground and to compute the downwelling clear sky radiances u_{L+1} and R received at level L+1 and at the ground, respectively. At the second step, MODTRAN2 was used to simulate the downwelling spectral radiance of the cloudy atmosphere R'. Note that for these simulations the multiscattering option was not utilized. The cirrus cloud model included in MODTRAN2 was selected because it offers enough flexibility to select the cloud altitude and thickness. To be consistent with the measurements, these parameters were set at 1.4 km and 0.4 km, respectively. In addition to altitude and thickness, the cirrus cloud option allows for the adjustment of the cloud IR transmittance through an absorption coefficient. With this capability, several simulated radiances have been generated for different cloud transmittances. These simulations were then used to test eqs. 7 and 9.

The results of the simulation tests are gathered in Fig. 7. The reference curve is defined as the "truth", which correspond to the temperature-transmittance input used in MODTRAN2 simulations. For comparison, the apparent temperature and cloud transmittance (9.3 μm) derived from the evaluation method are also shown in Fig. 7 (simulation points). As seen, the overall agreement between the two results is very good. At high transmittance level the cloud evaluation method slightly differs from the reference curve mainly because of certain limitations in the numerical accuracy of MODTRAN2 calculations. At worst, this corresponds to temperature errors smaller than 1 degree for transmittances higher than 80 %. Of less importance is an error introduced by the radiance model itself such as formulated in eq. 1. This equation is analytically exact only within the limits of a monochromatic radiation (infinite resolution). However, through a series of calculations, we have verified that eq. 1 can also be used to compute radiances at a moderate resolution of 1 cm^{-1} where the resulting
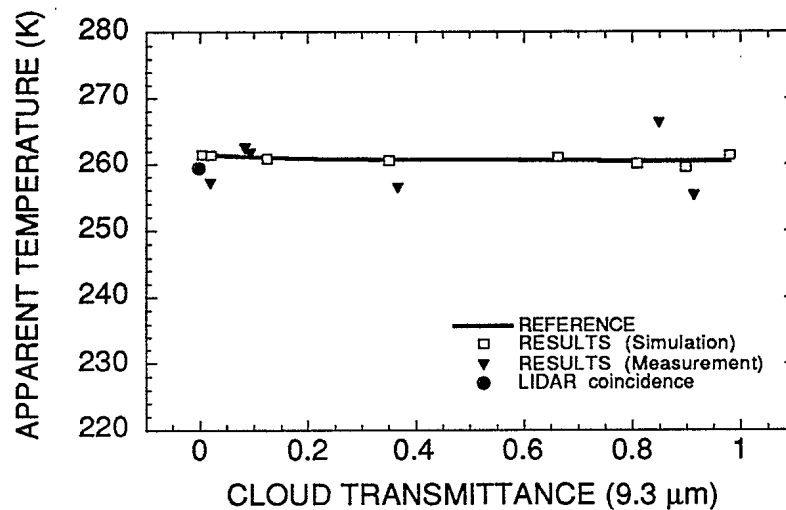
14

FIGURE 7 - Results of the cloud temperature-transmittance estimation method for different simulated and measured spectra corresponding to the 6 December 95
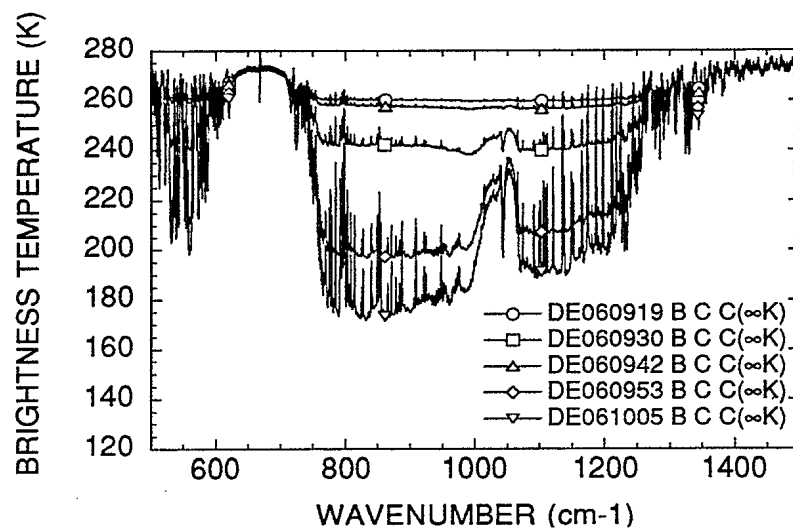

FIGURE 8 - Sequence of spectral radiance measurements in cloudy sky conditions recorded the 6 December 95 between 9:19 a.m. and 10:05 a.m.

15

numerical error appears to be negligible.

Secondly, the cloud evaluation method has been tested on a sequence of experimental spectra reported in Fig. 8. These spectral radiance measurements correspond to a decreasing cloudiness recorded on December 6th, 1995 between 9:19 a.m. and 10:05 a.m. The corresponding temperature and transmittance results appear in Fig. 7. In this case, the evaluation method gives the right order of magnitude, but there are differences of up to 6 K. The temporal variability of the cloud parameters with respect to the lidar sounding (height=1.4 km and thickness=0.4 km) is partly responsible for this discrepancy: For the time-coincident lidar measurement (round dot in Fig. 7), the temperature difference is smaller than 2 K. A remaining source of error may also be due to the fact that the actual line of sight of both sounding systems, the spectrometer and the lidar, was not exactly coincident. In this case the spatial variability of the cloud parameters may be the limiting factor. Unfortunately, with the actual setup, it was not possible to aim at exactly the same cloud area with the two instruments.

Finally, as stated earlier, a minor source of errors comes from the fact that the radiance measurements contain an additional contribution from the multiply scattered radiation in the cloud, while the evaluation method ignores this contribution. For the time being, there is no reliable radiative transfer model available to properly evaluate the multi-scattering effect in cloudy atmosphere: Recent versions of models such as MODTRAN and FASCODE offers multiscattering algorithm, but they have not been fully validated yet. However, simple arguments suggest that this multiscattering contribution would be negligible in the 9.3 μm region because the reflectance of cloud constituents (liquid water and ice crystal) is very small (approximately 1%, see Fig. 5), which tends to favor absorption rather than scattering in the extinction process.

5.2 Extension of the Method

The multiscattering effects and the parasite contribution from the earth radiation reflected from the cloud such as discussed in Section 4, remain two issues that should be addressed in further model developments. With a proper handling of these two radiance contributions it would be possible to extend the current model to the evaluation of cloud transmittance in the 10 to 12 μm region (800-1000 cm^{-1}). The proposed procedure of cloud

UNCLASSIFIED

16

evaluation in the context of an extended method can be summarized in the six following steps:

1- Evaluation of the cloud temperature and transmittance by eqs. 7 and 9,

2- Inversion of the lidar data to extract the mean radius of the cloud particles and the extinction coefficient,

3- Computation of both the multiscattering and the cloud-reflected radiance contributions (8-12 μm) from the inverted cloud parameters;

4- Correction of the measured spectral radiance to remove these two contributions (cloud-reflected and multiscattering);

5- Second application of eqs. 7 and 9 on the corrected radiance spectrum, but with an extension to other micro-windows found in the IR. This would allow for the determination of the cloud transmittance in the 800-1000 cm^{-1} region (8-10 μm). In this spectral domain, distinct optical properties of ice crystal and liquid water make transmittance sensitive to the nature of the cloud particles. In this case, the water / ice cloud ratio can be obtained from the shape of the spectral transmittance;

6- Computation of more accurate cloud-reflected and multiscattering radiance contributions using the results of step 5, generation of an updated correction for the measured radiance, and again application of eqs. 7 and 9 to improve the cloud temperature-transmittance determination.

The benefit of this iterative method of cloud evaluation based on spectral and lidar data is to provide all the microphysical information needed to model the radiative transfer throughout the visible up to the far infrared.

A fundamental application of this extended method is to help solving the often reported ambiguity concerning daytime radiance in the 1 to 4 μm region. In this case, the strong solar scattering on the cloud particles is poorly modelled by most of the available radiative transfer models. Factors of two between simulated and measured radiances are not uncommon in this spectral region. This is one of the main concerns of today's modelers. It is believed that the method of cloud evaluation based on the spectral and lidar data proposed in this report might constitute a powerful tool to support the development and validation of radiative transfer models for cloudy atmospheres.

UNCLASSIFIED

17

5.3 Impact of Background Profiles

An important aspect that needs to be addressed is the impact of background profiles used in the method for the calculations of clear sky radiance and transmittance data (R, u_{L+1} and τ_{L+1}). Figure 9 shows radiosonde recordings of temperature and humidity profiles for December 5th (clear day) and 6th (cloudy day), 1995. It is convenient to remember that the temperature-transmittance results shown in Fig. 7 were derived based on the exact profiles of the day of measurements (6 Dec. 95). The same format of results, but computed with approximate profiles (typical) rather than the exact ones (actual), appears in Fig. 10. The approximate profiles are simply those recorded the day before (5 Dec. 95) in clear sky conditions. As seen, the method is weakly sensitive to the input profiles. Even with errors of 10 K in the first kilometer for the temperature profile together with a level of humidity two times lower than the actual one, the induced errors in the cloud temperatures and transmittances are approximately 2 K and 4%, respectively.

This low sensitivity to the input profiles has the practical advantage that the cloud evaluation method can be utilized without supporting radiosondes. The previous example corresponds to an extreme scenario in which no additional effort was made to improve the profile estimates. In real situations, the ground level temperature and humidity are easily available. Thus, the application of a simple technique for scaling the rough profiles with ground level meteorological data would result in improved profile estimates. The temperature and humidity profiles can also be improved based on the radiance spectrum itself. For instance, in Ref. 6, a simple algorithm has been proposed to estimate the temperature profiles in the first 500 meters (above ground) using the spectral radiance in the CO_2 absorption band near 15 μm. Another practical example is the case of broken clouds. In this case, the downwelling spectral radiance from a clear portion of the sky can be inverted to retrieve the full temperature and humidity profiles as proposed in (Refs. 2 and 7). It is believed that, in operational scenarios and without a radiosonde, the systematic use of a simple technique for obtaining proper profile estimates can improve the cloud evaluation method to a level of approximately 1 K error in temperature and 2% in transmittance.

To further illustrate the potential of the method, Figs. 11 and 12 show another example in which the method has been applied to a sequence of radiance spectra recorded in the cloudy conditions of December 4th, 1995 (Fig. 11). There was no radiosonde available for this day. However, the ground temperature and humidity were very similar to the
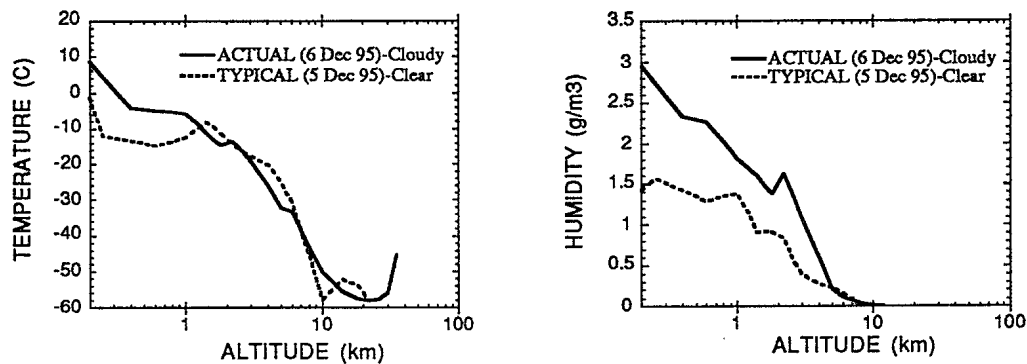
18

FIGURE 9 - Profiles of temperature and absolute humidity recorded (9:30 a.m.) by the radiosonde system for December 5th (clear sky) and 6th (cloudy sky), 1995
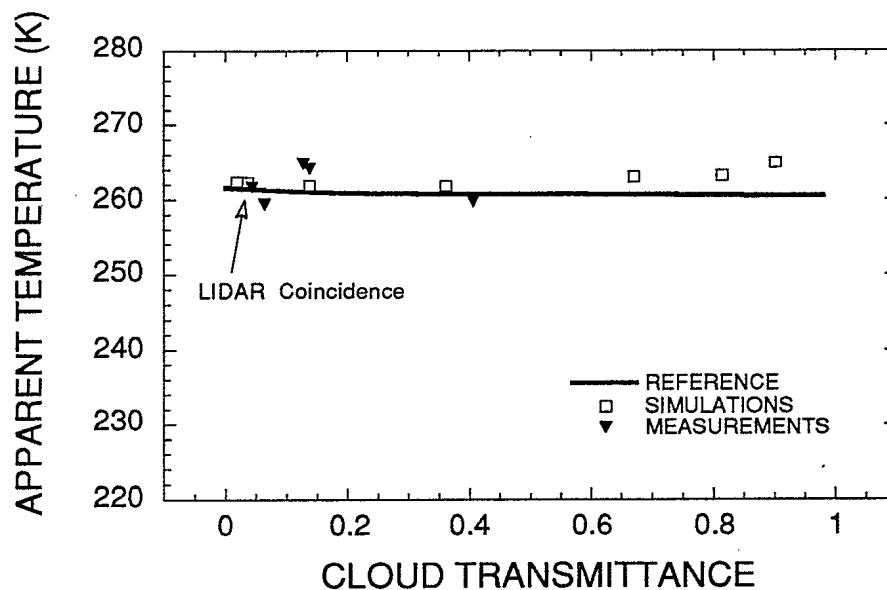
FIGURE 10 - Impact of the background profiles: The cloud temperature-transmittance estimation method is applied using typical profiles (5 December 1995) rather than the actual ones (6 December 1995) .
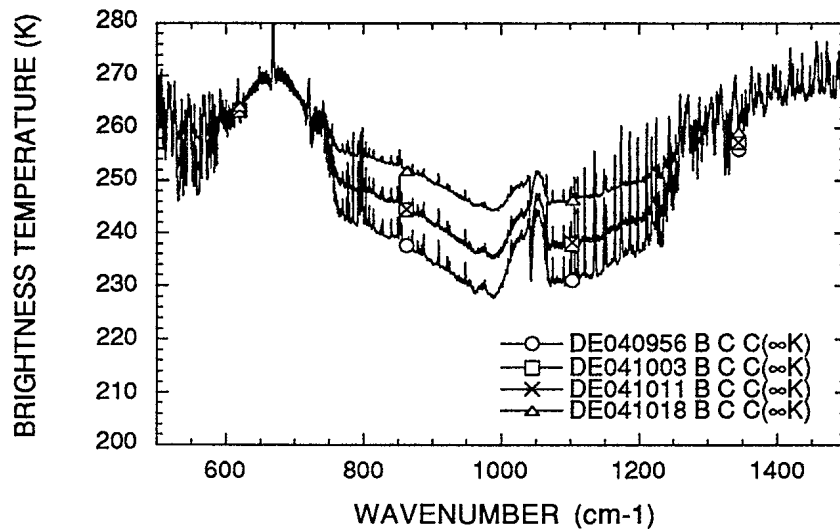
FIGURE 11 - Sequence of spectral radiance measurements in cloudy sky conditions recorded on December 4th, 1995 between 9:56 a.m. and 10:18 a.m.
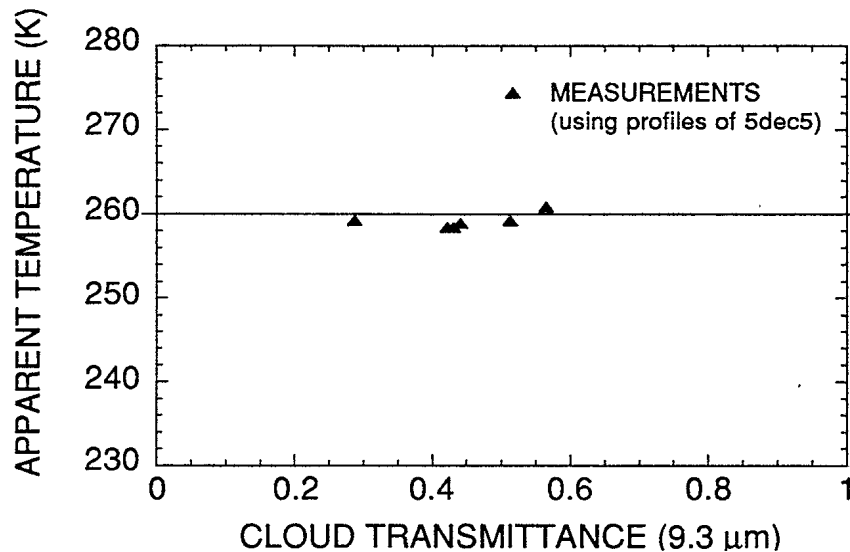

FIGURE 12 - Cloud temperature-transmittance estimations for a sequence of spectra recorded on December 4th, 1995

UNCLASSIFIED

20

ones recorded the following day (5 Dec. 95). For this reason, the radiosonde temperature and humidity profiles available for Dec. 5th were utilized as a good estimate to process the cloudy sky spectra of Dec. 4th. The results of the cloud evaluation are depicted in Fig. 12. As seen, for each spectrum of the sequence (9:56 a.m. to 10:18 a.m.), the cloud temperature is very stable and close to 259 K on the average, while transmittance varies by approximately a factor of two from 25% to 55%. Unfortunately, because of no radiosonde was available for this day, it was not possible to directly validate the cloud temperature evaluations.

However, in a preliminary study, the current multiscattering inversion algorithm of Bissonnette (Ref. 1) has been applied to the lidar data recorded concurrently with the spectral data. The result of the lidar inversion suggests that the average radius of the cloud particles is roughly equal to 2 μm, which leads to a cloud transmittance of approximately 2 % at the lidar wavelength (1.06 μm). This value of transmittance is in good agreement with the cloud opacity noted by visual observations. It also seems to contrast the high transmittance level found in the IR by the cloud evaluation method (Fig. 12). However, using simple arguments borrowed from the diffraction theory applied to spherical particles, it appears that the high values of cloud transmittance derived from spectral data at 9.3 μm (25-55%) are very consistent with cloud particle radius of 2 μm i. e. cloud transmittance results are in good agreement with what is expected from lidar data.

5.4 Impact of Ozone Variability

The last major source of possible limitations in the implementation of the cloud evaluation method is the variability of ozone concentration. For now, the method is based on the spectral contrast of the ozone emission near 9. 6 μm. Thus, to be accurate, it requires good knowledge of the ozone concentration. It is well known that the ozone profiles in the atmosphere are quite stable from time to time but they vary with the location and season. Usually, the ozone mixing ratios are properly accounted for by the six standard profiles: tropical, midlatitude summer, midlatitude winter, subarctic summer, subarctic winter and U. S. standard. These are the profiles included in MODTRAN that should be used in relation to the proposed cloud evaluation method. However, the industrial activities in and near the urban areas favor both the creation and destruction of ozone near the surface: Punctual measurements performed in polluted areas usually show variations of ozone concentration as important as 5 to 60 ppm over a period of a few hours with a repetitive cycle of
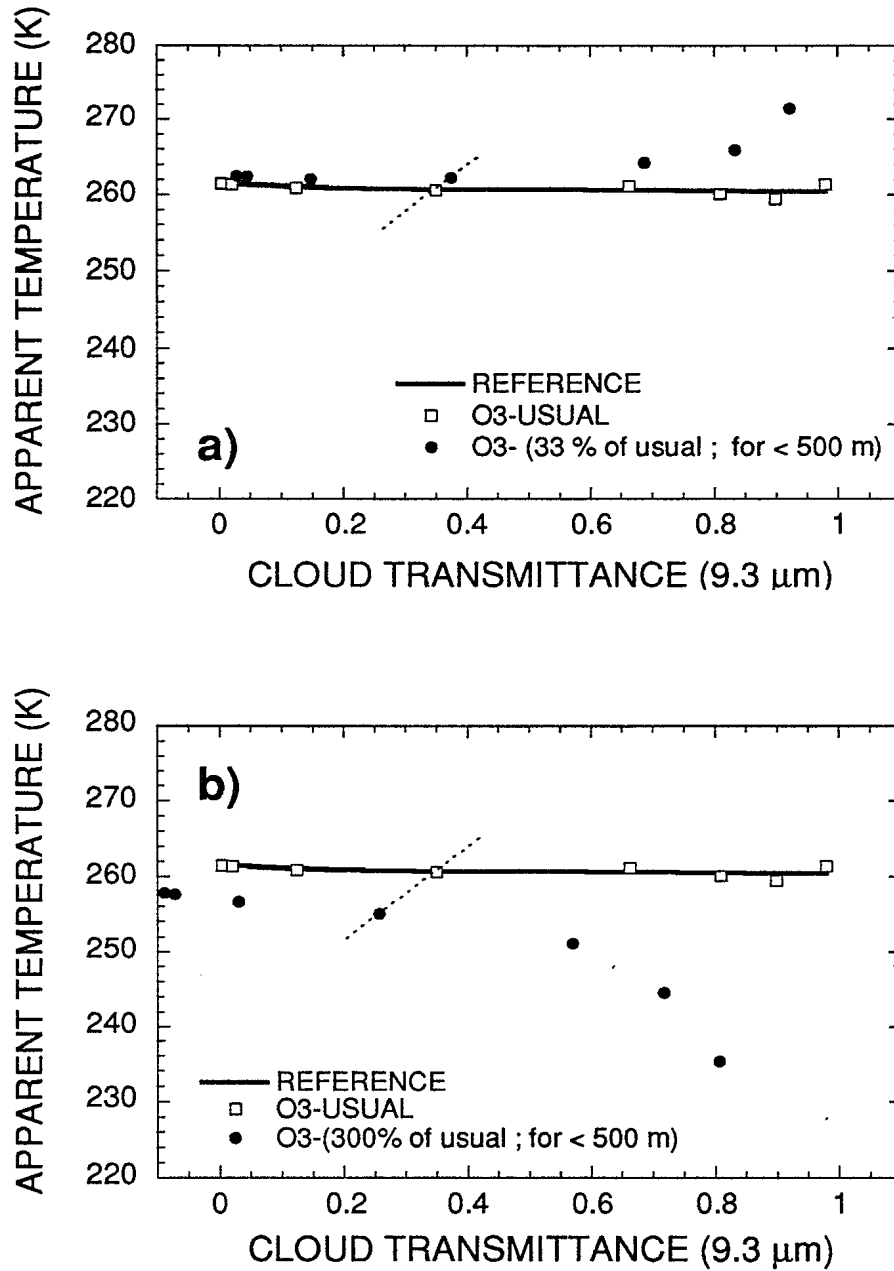
FIGURE 13 - Impact of ozone variability near the surface : a- the O_3-concentration is reduced to a third of the actual value in the first 500 m above the ground, while for b- it is increased to three times the actual value (< 500 m). For these calculations, the O_3 profile is kept equal to the default value for this location and season (midlatitude winter).

22

approximately 24 hours. These measurements are usually taken very close to the ground (approximately 3 m above), and to the best of our knowledge the characterization of the ozone variability in the first kilometer above the surface has not been addressed yet.

In order to estimate the impact of ozone variability near the surface, we have simulated the effect of erroneous ozone concentrations. Figure 13a represents the temperature-transmittance results obtained when the O_3 concentration is reduced to a third of an assumed typical value of 30 ppm in the first 500 meters above the ground. In Fig, 13b, the ozone concentration is three times the actual one. Overall, the impact is much more pronounced at high values of cloud transmittance. For cloud transmittances lower than approximately 50% the impact is not too severe: a 66% error in the ozone concentration (near the surface) yields cloud temperature errors smaller than 2 K and cloud transmittance errors of the order of 3%.

Finally, to cover all possible scenarios of cloud characterization, including urban areas, it might be requested to provide the method with information from a punctual sensor of ozone. However, over the last three years many clear sky measurements of the ozone emission band (near 9.6 µm) taken at DREV with the DBIS do not exhibit such large ozone variations as those recorded by the punctual sensors. This suggests that the ozone fluctuations near the surface appear in a layer thickness very much smaller than 500 m, which in this case should not seriously limit the accuracy of the cloud evaluation method.

6.0 SUMMARY AND CONCLUSIONS

A method for estimating the cloud temperature and transmittance from the downwelling spectral radiance has been proposed. The development of the method is supported by ground-based observations performed with a Fourier transform spectrometer system having a spectral resolution of 1 cm^{-1} and covering the IR band from 3 to 20 µm.

The basic principle of the method is simple. It uses of the strong emission band of ozone in the infrared. Because most of the ozone emission originates from the upper atmosphere, it constitutes a natural source of IR radiation for probing clouds in the lower part of the atmosphere using a ground-based receiver. Temperature and transmittance are derived from the cloudy sky radiance measured in two narrow spectral channels : one is in the ozone

UNCLASSIFIED

23

emission band at 9.48 μm and the second one is off the band at 9.15 μm. The choice of these channels simplifies the calculation because they are free of water vapor absorption lines. The solution for cloud temperature and transmittance is found by solving a system of two equations which requires, as input, an estimate of the cloud height and thickness obtained from lidar returns, and an estimate of atmospheric temperature and humidity profiles to simulate the background atmosphere from MODTRAN calculations.

The method has been tested in two different ways. The first validation was done to verify the impact of the few assumptions behind the method. For that a series of simulations were performed with the atmospheric model MODTRAN2 using the cirrus cloud option. These simulations indicate that temperature errors introduced by the approximations are always smaller than 1 K for any cloud transmittance. The second validation was done on a selected series of experimental spectra. In this case, the evaluation method gives quite accurate results with typical temperature errors smaller than 2 K for spectral measurements coincident in time with the lidar measurements. The main part of the remaining error has been attributed to the imperfect boresighting of the spectrometer and lidar systems.

The study is completed by an analysis of the two main sources of limitation that might be encountered in the application of the method. The first limitation is related to the accuracy of background temperature and humidity profiles required by the method. Results of this analysis indicate a weak sensitivity to input profiles: Even with errors of 10 K in the first kilometer of the temperature profile, coupled to an error of a factor of two in the humidity profile the resulting errors in cloud temperature and transmittance are usually smaller than 2 K and 4%, respectively. This low sensitivity to input profiles has the great practical advantage that the cloud evaluation method can be utilized without supporting radiosondes. The second source of potential limitation is due to the time variability of ozone concentration. Through a series of simulations the impact of the ozone variability in the first 500 m of the atmosphere above ground has been found to be not too severe: For cloud transmittance lower than 50 % an error of 66 % in ozone concentration near the surface leads to temperature errors smaller than 2 K and cloud transmittance errors of the order of 3 %. This level of accuracy can be further improved by adding a punctual ozone sensor to the actual instrumentation: spectrometer and lidar systems.

Next activities will be oriented to generalizing the cloud evaluation method to any slant path from the ground or from an airborne platform. A particular emphasis will be put

on evaluating the impact of multiple scattering on cloud temperature and transmittance determinations. An alternate method which uses two pure water vapor continuum microwindows to get ride of the ozone variability constraint will be investigated. Theoretical refinements of the method are also required to support wider spectral channels potentially usable in a simplified portable instrument, a two-band cloud radiometer.

This report provides a basis to further develop the cloud evaluation method for applications in icing hazard detection. The ultimate goal is to demonstrate that combined lidar and spectral measurements can be used for determining the temperature, the concentration and the composition (ice crystals or supercooled water droplets) of clouds.

7.0 ACKNOWLEDGEMENTS

UNCLASSIFIED

25

8.0 REFERENCES

1. Bissonnette, L. and Hutt, D. L., "Multiply Scattered Aerosol Lidar Returns: Inversion Method and Comparison with in situ Measurements", Appl. Opt. 34, 6959-6975, 1995.

2. Thériault, J.-M., "Remote Sensing of Atmospheric Profiles Using Infrared Emission Spectra: Formulation of a Method", DREV R-4776 / 94, May 1994, UNCLASSIFIED

3. Rasmussen, R., Politovich, M., Marwitz, J., Sand, W., McGinley, J., Smart, J., Pielke, R., Rutledge, S., Wesley, D., Stossmeister, G., Bernstein, B., Elmore, K., Powell, N., Westwater, E., Stankov, B. B. and Burrows, D., "Winter Icing and Storms Project (WISP)", Bull. Am. Met. Soc., Vol. 73, 951, 1992.

4. Thériault, J.-M., Giroux, J., Côté, J., Fournier, M., Anderson, G. P. and Chetwynd, J. H., " The Double Beam Interferometer Sounder (DBIS): A Device for the Passive Remote Sensing of Atmospheric Profiles", Proceedings of the 1992 Battlefield Atmospheric Conference, Fort Bliss, El Paso, Texas, Dec. 1-3, pp. 91-100, 1992.

5. Anderson, G. P., Clough, S. A., Kneizys, F. X.,Shettle, E. P.,Chetwynd J. H. and Abreu, L. W., "FASCOD3 Update", Proceedings, 12th Annual Review Conference on Atmospheric Transmission Models, Geophysics Laboratory, Hanscom AFB, MA: 163, 1989.

6. Thériault, J.-M., Moncet, J.-L. and Bradette, C., "Spectral Sensing of IR Atmospheric Parameters", Proceedings of the European Symposium on Satellite Remote Sensing, Italy, Vol. 2312, pp. 10, 1994.

7. Thériault, J.-M, Anderson, G. P., Chetwynd, J. H., Murphy, E. P., Turner, V., Cloutier, M., Smith, A. and Moncet, J. L., "Retrieval of Tropospheric Profiles from IR Emission Spectra: Preliminary results with the DBIS", Conference on High Latitude Optics, European Optical Society / SPIE, Norway, pp. 10, July 1993.

UNCLASSIFIED

26

<u>INTERNAL DISTRIBUTION</u>

<u>DREV R-9608</u>

1 -   Deputy Director General
1 -   Chief Scientist
6 -   Document Library
1 -   J.-M. Thériault (author)
1 -   R. Larose
1 -   J.-M. Garneau
1 -   C. Carrier
1 -   L. Bissonnette
1 -   J. Cruickshank
1 -   P. Chevrette
1 -   J. Boulter
1 -   D. Dion
1 -   T. Smithson
1 -   J. Dubois
1 -   G. Roy
1 -   D. Hutt
1 -   Maj. F. Beaupré
1 -   C. Bradette
1 -   G. Vallée
1 -   C. Bastille
1 -   L. Durand

UNCLASSIFIED

27

UNCLASSIFIED

28

<u>EXTERNAL DISTRIBUTION (cont'd)</u>

<u>DREV R-9608</u>

1- Dr. B.D. Billard
   Naval Surface Warfare Center
   White Oak Laboratory
   Code R42
   Silver Spring, MD 20903-5000
   U.S.A.

1 - Dr. T. Jones
   U.S. Army Night Vision & Electro-optics
   Laboratory
   DELNV-VI
   Fort Belvoir, VA 22060
   U.S.A.

1 - Mr. R.K. Redfield
   Department of the Army
   Cold Regions Research & Engineering
   Laboratory
   Corps of Engineers
   Hanover, NH 03755
   U.S.A.

1 - Mr. N. Tolliday
   DRA (Funtington)
   Cheesmans Lane, Hambrook
   Near Chichester, W. Sussex
   U.K.

1 - Dr. O.G. Nielsen
   Danish Defence Research Establishment
   Osterbrogades Kaserne
   Dk 2100 Copenhagen 0
   Denmark

1 - M. A.P. Junchat
   CELAR-Centre d'électronique d'armement
   Division ASRE
   35170 Bruz
   France

1 - Dr. A. Kohnle
   Forschungsinstitut für Optik (FfO)
   Schloss Kressbach
   74 Tübingen
   Federal Republic of Germany

29

EXTERNAL DISTRIBUTION (contd)

DREV R-9608

3 -   Dr. A. Van Eijk, Dr. G. de Leeuw
        & Dr. G. J. Kunz
        Physics Laboratory FEL-TNO
        Oude Wallsdorperweg 63
        2597 AK, The Hague
        Netherlands

3 -   Dr. A. Van Eijk, Dr. G. de Leeuw
        & Dr. G. J. Kunz
        Physics Laboratory FEL-TNO
        Oude Wallsdorperweg 63
        2597 AK, The Hague
        Netherlands

1 -   Dr. G. Burfield
        Surveillance Research Laboratory
        Optoelectronics Division
        P.O. Box 1650
        Salisbury
        South Australia 5108
        Australia

UNCLASSIFIED
SECURITY CLASSIFICATION OF FORM
(Highest classification of Title, Abstract, Keywords)

DOCUMENT CONTROL DATA

1. ORIGINATOR (name and address) DREV, P.O. BOX 8800 Courcelette, Quebec G0A 1R0 ≉	2. SECURITY CLASSIFICATION (Including special warning terms if applicable) UNCLASSIFIED

3. TITLE (Its classification should be indicated by the appropriate abbreviation (S,C,R or U)

Remote Determination of Cloud Temperature and Transmittance from Spectral Radiance Measurements: Method and Results

4. AUTHORS (Last name, first name, middle initial. If military, show rank, e.g. Doe, Maj. John E.)

Thériault, Jean-Marc

5. DATE OF PUBLICATION (month and year)	6a. NO. OF PAGES	6b. NO. OF REFERENCES

7. DESCRIPTIVE NOTES (the category of the document, e.g. technical report, technical note or memorandum. Give the inclusive dates when a specific reporting period is covered.)

Technical Report

8. SPONSORING ACTIVITY (name and address)

9a. PROJECT OR GRANT NO. (Please specify whether project or grant)	9b. CONTRACT NO. 03D03-15
10a. ORIGINATOR'S DOCUMENT NUMBER R-9608	10b. OTHER DOCUMENT NOS. N/A

11. DOCUMENT AVAILABILITY (any limitations on further dissemination of the document, other than those imposed by security classification)

[X] Unlimited distribution
[ ] Contractors in appoved countries (specify)
[ ] Canadian contractors (with need-to-know)
[ ] Government (with need-to-know)
[ ] Defence departments
[ ] Other (please specify) :

12. DOCUMENT ANNOUNCEMENT (any limitation to the bibliographic announcement of this document. This will normally correspond to the Document Availability (11). However, where further distribution (beyond the audience specified in 11) is possible, a wider announcement audience may be selected.)

Unlimited

UNCLASSIFIED
SECURITY CLASSIFICATION OF FORM

13.   ABSTRACT (a brief and factual summary of the document. It may also appear elsewhere in the body of the document itself. It is highly desirable that the abstract of classified documents be unclassified. Each paragraph of the abstract shall begin with an indication of the security classification of the information in the paragraph (unless the document itself is unclassified) represented as (S), (C), (R), or (U). It is not necessary to include here abstracts in both official languages unless the text is bilingual).

This report presents a method for the evaluation of cloud temperature and IR transmittance (9.3 μm) from ground-based measurements of the the downwelling spectral radiance measured in cloudy conditions. The temperature and the transmittance are derived from radiances measured in two narrow spectral channels at 9.15 μm and 9.48 μm. Cloud parameters are found by solving a system of equations requiring as inputs, an estimate of the cloud height and thickness obtain from lidar returns, and an estimate of atmospherics temperature and humidity profiles. Validation tests performed on experimental spectra demonstrate the accuracy of the method with typical temperature errors smaller than 2 K for spectral measurements coincident in time with the lidar measurements.

14.   KEYWORDS, DESCRIPTORS or IDENTIFIERS (technically meaningful terms or short phrases that characterize a document and could be helpful in cataloguing the document. They should be selected so that no security classification is required. Identifiers, such as equipment model designation, trade name, military project code name, geographic location may also be included. If possible keywords should be selected from a published thesaurus. e.g. Thesaurus of Engineering and Scientific Terms (TEST) and that thesaurus-identified. If it is not possible to select indexing terms which are Unclassified, the classification of each sould be indicated as with the title.)

Passive Remote Sensing

Infrared Spectra

Cloud Temperature

Cloud Transmittance

FTIR Spectrometer

Icing Hazard Detection

500380

(DCD03E.IFD - 95.02.22)